Journal of Alloys and Compounds 502 (2010) 180–183

Contents lists available at ScienceDirect

Journal of Alloys and Compounds

journal homepage: www.elsevier.com/locate/jallcom

Afterglow phosphor materials Y_2O_2S: Eu, Mg, Ti doped with various Gd concentrations

Tongkun Ji [a], Hongyi Jiang [a,*], Fei Chen [b]

[a] School of Materials Science and Engineering, Wuhan University of Technology, Wuhan 430070, PR China
[b] Key Laboratory of Advanced Technology for Specially Functional Materials, Ministry of Education, Wuhan University of Technology, Wuhan 430070, PR China

ARTICLE INFO

Article history:
Received 5 January 2010
Received in revised form 15 April 2010
Accepted 17 April 2010
Available online 15 May 2010

Keywords:
Phosphors
X-ray diffraction
Solid state reaction
Luminescence

ABSTRACT

Red afterglow phosphors Y_2O_2S with 5 mol% Eu, 2 mol% Mg, 4 mol% Ti (fixed) and various Gd ion concentrations (0–3 mol%) were prepared by solid state reaction method. The phase compositions of the obtained phosphor were characterized by powder X-ray diffraction (XRD) method. The surface morphology and the particle size were observed by scanning electron microscopy (SEM). Luminescent properties were investigated by measuring emission spectra, excitation spectra and decay curves. The results indicated that the major phase with various doped Gd ion concentrations was not changed, the intense red emission was observed for the Y_2O_2S: Eu, Mg, Ti, Gd phosphor (λ_{max} = 626 nm). The Gd ion doping may change the trap depth in the Y_2O_2S matrix and improve the luminescent properties of the samples. The optimized Gd ion concentration of the red afterglow phosphor is 1 mol%. The stability of the phosphor with respect to the air and humidity were also explored.

1. Introduction

Long afterglow phosphor is a kind of important optical functional materials which can emit visible light for a long time in darkness after excited by the sunlight, UV (ultraviolet) lamp or fluorescence lamp. Even after the light source is turned off, the afterglow of the phosphor will last for several minutes or tens of hours. The blue and green afterglow phosphors with high brightness and long afterglow time have been prepared successfully [1–4]. However, the red afterglow phosphor with better luminescent property is difficult to achieve. Many researchers have done a lot of works to improve the luminescent properties of red phosphors in recent years. Various red afterglow phosphors were synthesized successfully, including CaS [5], $CaTiO_3$ [6–8], $Sr_3Al_2O_6$ [9–11], Gd_2O_2S [12] and Y_2O_2S [13].

The red afterglow phosphor Y_2O_2S: Eu, Mg, Ti which has high initial brightness and long afterglow time (over 3 h) has attracted more attentions since 1999 reported by Murazaki et al. [14]. Since then, the Y_2O_2S: Eu, Mg, Ti phosphor has been extensively investigated. Wang et al. [15] investigated the effect of various sintering atmospheric conditions on the crystalline phase and luminescent properties of Y_2O_2S: Eu, Mg, Ti. Zhang et al. [16] synthesized the Y_2O_2S: Gd, Eu, Ti, Mg phosphor by a gas absorption method and studied the effect of Ti^{4+} and Mg^{2+}ions doping on the luminescent properties. Wang and Wang [17] synthesized the Y_2O_2S: Eu, Ti, Mg phosphor by flux method and investigated the relation between the luminescent properties and the crystal structures. Hölsä et al. [18] studied the emission and excitation in the visible and UV-VUV lights of the Y_2O_2S: Eu, Mg, Ti phosphor. Liu and co-workers [13] reported on an effective method to synthesize Y_2O_2S: Eu, Ti, Mg nanoparticles. Although the Y_2O_2S: Eu, Mg, Ti phosphor is currently one of the best red afterglow materials, its luminescent property is worse than that of the blue and green phosphors. Therefore, it is significant to further improve the luminescent properties of the Y_2O_2S: Eu, Mg, Ti red afterglow phosphor for advanced and practical applications.

Recently, the effect of co-doping for substantial extension of the spectral emission range to form the white light emitting diodes is widely used [19,20]. It is shown that doping may stimulate the emission properties due to excited absorption, up-conversion and energy transfer, which is also an effective way to improve the luminescent properties of the long afterglow phosphors. Zeng et al. [21] reported the luminescent properties of Si^{4+} and Zn^{2+} co-doped Y_2O_2S: Eu phosphor and found the doping of Si^{4+} and Zn^{2+} ions could prolong the afterglow time remarkably. Yuan et al. [22] reported the effect of doping with Mg, Ti, Ba, Ca and Sr ions on the luminescent properties of Y_2O_2S: Eu phosphor. Guo et al. [23] reported the enhancement mechanism of luminescent properties of RE^{3+} (RE^{3+} = Eu^{3+}, Sm^{3+}, Dy^{3+}) in Y_2O_2S phosphor by a trace of Tb^{3+}. Aizawa et al. [24] reported the $SrAl_2O_4$:Eu^{2+} phosphor doped with Nd, Sm, Lu, Gd, Dy and Y, and found that the long afterglow phosphorescence was influenced by the depth and density of the traps. Chen et al. [1] reported that the luminescent properties of $SrAl_2O_4$:Eu^{2+}, Dy^{3+} could be significantly modified by the Yb^{3+} ions

* Corresponding author. Tel.: +86 27 87651772; fax: +86 27 87642079.
E-mail addresses: tongkunji@whut.edu.cn (T. Ji), jianghy@whut.edu.cn (H. Jiang).

0925-8388/$ – see front matter © 2010 Elsevier B.V. All rights reserved.
doi:10.1016/j.jallcom.2010.04.139

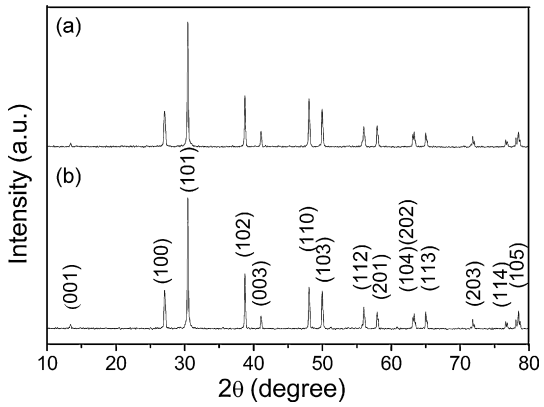

Fig. 1. XRD powder patterns for phosphors sintered at 1250 °C for 3 h: (a) $Y_{1.89}O_2S$: $Eu_{0.05}$, $Mg_{0.02}$, $Ti_{0.04}$; (b) $Y_{1.88}O_2S$: $Eu_{0.05}$, $Mg_{0.02}$, $Ti_{0.04}$, $Gd_{0.01}$.

doping. Ryu and Bartwal [2] investigated the optimization of Dy^{3+} doping in $CaAl_2O_4$:Eu phosphor.

In this study, the effect of Gd ion doping on the luminescent properties of long afterglow phosphor Y_2O_2S: Eu, Mg, Ti was investigated. The XRD, SEM, emission spectra, excitation spectra and decay curves were used to characterize the obtained phosphors. The stability of the phosphor with respect to the air and humidity was investigated and the mechanism for the improvement of the luminescent properties was also explored.

2. Experimental procedures

$Y_{1.89-x}O_2S$: $Eu_{0.05}$, $Mg_{0.02}$, $Ti_{0.04}$, Gd_x phosphor with various Gd ion concentrations (x = 0, 0.5, 1 and 3 mol%) was prepared by solid state reaction method. The raw materials used were Y_2O_3 (99.999%), Eu_2O_3 (99.99%), MgO (98.5%), TiO_2 (98%), Gd_2O_3 (99.95%), Na_2CO_3 (99.8%) and sulfur (99.5%) powders. Firstly, Na_2CO_3 and sulfur were mixed as a flux. The molar ratio of Y_2O_3:Na_2CO_3:S was 1:0.68:2. The raw materials were weighed, well mixed in agate mortar, pressed into disc pellets, and sintered at 1250 °C for 3 h in a graphite crucible with a lid in a weak reducing ambient. The as-sintered phosphors were washed with 1 mol/L nitric acid, followed by being washed in hot pure water at 80 °C in order to remove the residual sulfur and so on. And then, the obtained phosphors were heated at 600 °C for 1 h in air to remove the graphite. In order to investigate the stability of the obtained phosphors with respect to humidity, the synthesized powder was socked in pure water at room temperature for 30 days, and then it was dried at 80 °C. In order to study the thermal stability of the obtained phosphor in air, the phosphors with suitable quality were heated in the temperature range of 200–1000 °C for 30 min in air and cooled down to room temperature.

After sieving though a 120 mesh sieve, the phase compositions of the synthesized phosphor were detected by X-ray diffraction (XRD) method which were conducted on a Rigaku D/max–IIIA X-ray diffractometer, operating at 35 kV and 30 mA with a scan speed of 10°/min and a step of 0.02° using Cu K_α radiation (λ = 1.54056 Å). The surface morphology and the particle size were observed by JSM-5610LV (Japan) operating at 25 kV. The excitation and emission spectra of obtained phosphors were obtained by a Hitachi F-4500 fluorescence spectrometer and 150 W Xe-lamp as the excitation source, the spectral resolution was maintained at 1 nm for both excitation and emission, and the PMT Voltage was set at 700 V. The decay curves of afterglow phosphors were measured by the ST-86LA brightness meter, the samples were irradiated by ultraviolet lamp (365 nm) for 10 min after the brightness had declined lower than 9 mcd/m^2. All the above measurements were carried out at room temperature.

3. Results and discussion

Fig. 1 shows the XRD patterns of $Y_{1.89-x}O_2S$: $Eu_{0.05}$, $Mg_{0.02}$, $Ti_{0.04}$, Gd_x phosphors with various Gd ion concentrations (x = 0 and 1 mol%) prepared at 1250 °C for 3 h. It can be seen that the major phase matches well with the JCPDS date file (no. 24-1424). No other phase or unreacted material was detected. The co-doped Eu, Mg, Ti and Gd ions have little influence on the structure of the host material. The radius of Gd^{3+} ion (0.94 Å) is slightly larger than that of Y^{3+} (0.89 Å), and the Gd^{3+} ion is expected to occupy the Y^{3+} site in Y_2O_2S matrix.

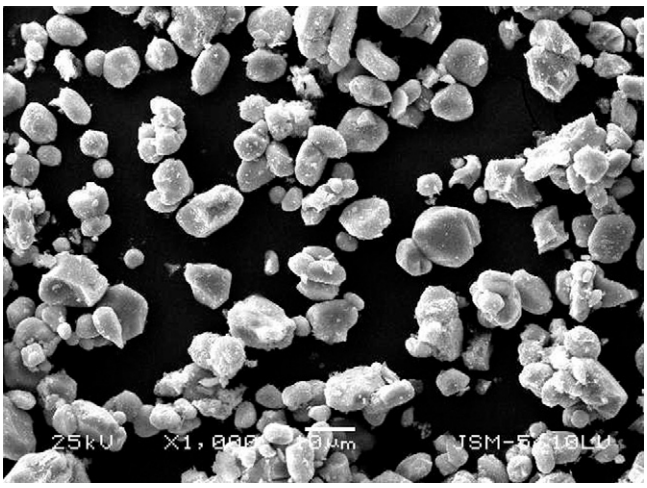

Fig. 2. The SEM micrograph for $Y_{1.88}O_2S$: $Eu_{0.05}$, $Mg_{0.02}$, $Ti_{0.04}$, $Gd_{0.01}$ sample.

Fig. 2 shows the SEM micrograph for $Y_{1.88}O_2S$: $Eu_{0.05}$, $Mg_{0.02}$, $Ti_{0.04}$, $Gd_{0.01}$ composition. As can be seen from Fig. 2, the elliptic and polyhedral shapes of particles were observed, and the sizes of particles are ranging from 3 to 10 μm.

The emission spectra of $Y_{1.89-x}O_2S$: $Eu_{0.05}$, $Mg_{0.02}$, $Ti_{0.04}$, Gd_x phosphors with various Gd ion concentrations are shown in Fig. 3. The samples were excited by 345 nm light. It can be seen from Fig. 3 that the emission spectrum of $Y_{1.89}O_2S$: $Eu_{0.05}$, $Mg_{0.02}$, $Ti_{0.04}$ has the strongest peak at 626 nm which is attributed to the $^5D_0 \rightarrow {}^7F_2$ transitions of Eu^{3+}. The other peaks are located in the range of 460–613 nm due to the ^5D_J (J = 0, 1, 2) → ^7F_J (J = 0, 1, 2, 3) transitions of Eu^{3+}. Moreover, broad emissions are clearly observed from the obtained spectra, indicating a strong electron–phonon interaction, which has been reported in the literature [25,26].

Compared with the phosphor $Y_{1.89}O_2S$: $Eu_{0.05}$, $Mg_{0.02}$, $Ti_{0.04}$, the emission spectra of $Y_{1.89-x}O_2S$: $Eu_{0.05}$, $Mg_{0.02}$, $Ti_{0.04}$, Gd_x with various Gd ion concentrations have similar emission peak position and patterns except the intensity. When the phosphor is doped with 1 mol% Gd and 5 mol% Eu, 2 mol% Mg and 4 mol% Ti, the intensity of observed emission spectra reaches the maximum value. When the Gd ion concentration is over 1 mol%, the emission intensity value is decreased. The decay time of the phosphor with 1 mol% Gd is also better than that of other combinations. Thus, the optimized Gd ion concentration is 1 mol%.

The excitation spectra for $Y_{1.89-x}O_2S$: $Eu_{0.05}$, $Mg_{0.02}$, $Ti_{0.04}$, Gd_x with various Gd ion concentrations in the range of 200–450 nm is shown in Fig. 4. Two broad excitation peaks centered at 256 and 310 nm are observed when monitored at 626 nm. The peak at

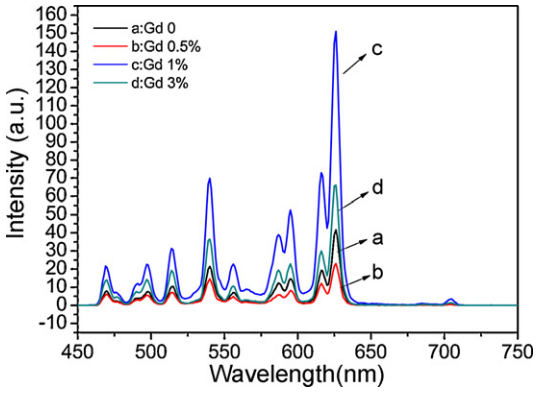

Fig. 3. Emission spectra for $Y_{1.89-x}O_2S$: $Eu_{0.05}$, $Mg_{0.02}$, $Ti_{0.04}$, Gd_x (x = 0, 0.5, 1 and 3 mol%) samples.

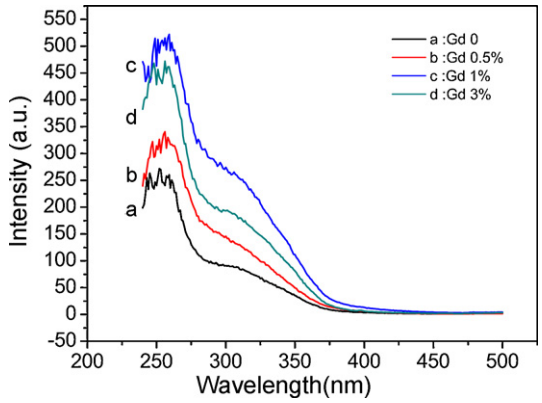

Fig. 4. Excitation spectra for $Y_{1.89-x}O_2S$: $Eu_{0.05}$, $Mg_{0.02}$, $Ti_{0.04}$, Gd_x (x = 0, 0.5, 1 and 3 mol%) samples.

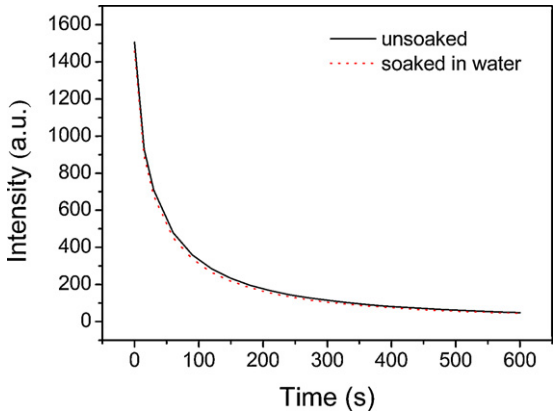

Fig. 6. Decay curve of Y_2O_2S: Eu, Mg, Ti, Gd (1 mol% Gd) phosphors socked in pure water and unsocked.

256 nm is attributed to O-Eu charge transfer states (CTS). The peak found at 310 nm is due to the S-Eu or Ti-Eu CTS. The excitation spectra are similar with the results of other reports [16,27]. It is clearly seen that the intensity of excitation spectra is greatly improved with increase in the Gd ion concentrations. When the phosphor is doped with 1 mol% Gd, the intensity of observed excitation spectra reaches the maximum value. When the Gd ion concentration is over 1 mol%, the intensity is decreased. Thus, it is also suggested that the optimized Gd ion concentration is 1 mol%, which is in agreement with the emission spectra results.

The decay curves of $Y_{1.89-x}O_2S$: $Eu_{0.05}$, $Mg_{0.02}$, $Ti_{0.04}$, Gd_x (x = 0, 0.5, 1 and 3 mol%) phosphors are shown in Fig. 5. The decay time was measured after the phosphors were activated by UV lamp at room temperature for 10 min. It can be seen that all the obtained phosphors show a sharp decrease and then a stable long persistent process for several hours. However, the phosphor shows different afterglow properties with different Gd ion concentrations. The afterglow times of samples with Gd doping are longer than the undoped one. When the Gd ion concentration is 1 mol%, the obtained afterglow phosphor $Y_{1.88}O_2S$: $Eu_{0.05}$, $Mg_{0.02}$, $Ti_{0.04}$, $Gd_{0.01}$ exhibits the highest initial brightness and the longest afterglow time. On the other hand, when the Gd ion concentration is over 1 mol%, both the initial brightness and the afterglow time of the phosphor are decreased. Thus, it is implied that the Gd doping on the Y_2O_2S matrix has great effects on the luminescent properties of the observed phosphors.

The decay curve of Y_2O_2S: Eu, Mg, Ti, Gd (1 mol% Gd) phosphor socked in pure water is shown in Fig. 6. Compared with the unsocked one, the luminescent property is changed very little.

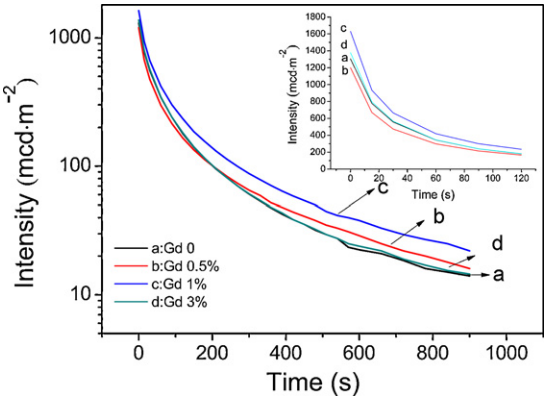

Fig. 5. Decay curves for $Y_{1.89-x}O_2S$: $Eu_{0.05}$, $Mg_{0.02}$, $Ti_{0.04}$, Gd_x (x = 0, 0.5, 1 and 3 mol%) phosphors. Inset graph shows the decay curves at the beginning time (0–120 s).

Therefore, it is clear that the phosphor is stable in moist environment (even in water) for 30 days.

Fig. 7 shows the decay curves for Y_2O_2S: Eu, Mg, Ti, Gd (1 mol% Gd) phosphors heated in air at different temperatures for 30 min. It is indicated that the luminescent property is not changed remarkably after the phosphor heated in air before 600 °C. After the phosphor was heated at 800 °C for 30 min, the intensity degradation is slow and the relative luminescent intensity (after the excitation source turned off for 5 min) of the phosphor is decreased only to 80% compared with that of unheated one. When the heating temperature is increased to 1000 °C, the intensity degradation is very fast and shows no afterglow phenomenon. So, it can be seen that the Y_2O_2S: Eu, Mg, Ti, Gd (1 mol% Gd) phosphor is stable in air at room temperature.

According to the above results, it can be seen that the Y_2O_2S: Eu, Mg, Ti, Gd phosphor has good stability with respect to the air and humidity.

There are many reports about the mechanism of the long afterglow phosphor [28–31]. However, the detailed process of long afterglow phenomenon is still not clear. The thermo-stimulated recombination of holes and electrons is generally accepted at present. After excited by light source, free holes and electrons are formed in the host material. The holes and electrons can be trapped by defect centers, and then released back to meta-stable state thermally and recombined with opposite charges at the luminescent centers resulting light emission for a long time. The traps with suitable depth are related to the long afterglow phenomena. If the trap depth is too deep, the holes or electrons trapped in the defect

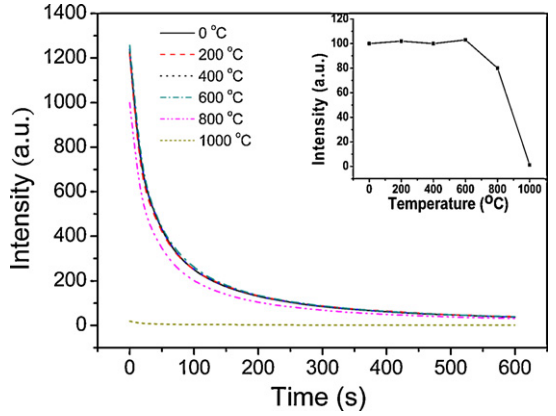

Fig. 7. Decay curves for Y_2O_2S: Eu, Mg, Ti, Gd (1 mol% Gd) phosphors heated in air at different temperatures. Inset graph shows the relative luminescent intensity at 5 min.

centers are difficult back to meta-stable state at room temperature. If the trap depth is too shallow, the trap releases the holes or electrons quickly, and results in short afterglow time. So, only the phosphor with suitable depth traps gives the best luminescent properties.

Liu and Che [32] reported that the luminescent properties of Y_2O_2S phosphor were greatly enhanced when doped with Gd ion due to the enhancement of intensity for thermoluminescence (TL) spectrum at 345 K. The result revealed that the introduction of Gd ion changed the traps in the host matrix. So it is concluded that the introduction of Gd ion into the Y_2O_2S: Eu, Mg, Ti may also change the traps and make the trap depth more suitable for the Y_2O_2S: Eu, Mg, Ti phosphor. This may be the reason why Gd doping can improve the luminescent properties of Y_2O_2S: Eu, Mg, Ti phosphor. When Gd ion concentration is over 1 mol%, both the initial luminescence brightness and the afterglow time of the phosphor are decreased. The reason may be that the concentration more than the optimized value causes deeper trap depth. The trap with deeper depth neutralizes the hole-electron recombination process, therefore, reduces the luminescent properties of Y_2O_2S: Eu, Mg, Ti, Gd.

4. Conclusions

New red afterglow phosphor materials Y_2O_2S: Eu, Mg, Ti doped with various Gd ion concentrations were synthesized successfully by solid state reaction method. The powder XRD indicates that the compositions are hexagonal phase. SEM images show that the elliptic and polyhedral particles are in the range of 3–10 μm. The doping with Gd ion has great effects on the luminescent properties. It is found that the optimized Gd ion concentration for the phosphor is 1 mol% when fixed the concentration of 5 mol% Eu, 2 mol% Mg and 4 mol% Ti. The Y_2O_2S: Eu, Mg, Ti, Gd phosphor shows good stability with respect to the air and humidity.

References

[1] R. Chen, Y. Wang, Y. Hu, Z. Hu, C. Liu, J. Lumin. 128 (2008) 1180.
[2] H. Ryu, K.S. Bartwal, J. Alloys Compd. 476 (2009) 379.
[3] C. Liu, Y. Wang, Y. Hu, R. Chen, F. Liao, J. Alloys Compd. 470 (2009) 473.
[4] X. Teng, W. Zhuang, Y. Hu, C. Zhao, H. He, X. Huang, J. Alloys Compd. 458 (2008) 446.
[5] Y. Kojima, T. Toyama, J. Alloys Compd. 475 (2009) 524.
[6] R. Chen, F. Song, D. Chen, Y. Peng, Powder Technol. 194 (2009) 252.
[7] T. Li, M. Shen, L. Fang, F. Zheng, X. Wu, J. Alloys Compd. 474 (2009) 330.
[8] W. Tang, D. Chen, Phys. Status Solidi (a) 206 (2009) 229.
[9] P. Zhang, L. Li, M. Xu, L. Liu, J. Alloys Compd. 456 (2008) 216.
[10] S.K. Sharma, S.S. Pitale, M.M. Malik, M.S. Qureshi, R.N. Dubey, J. Alloys Compd. 482 (2009) 468.
[11] C. Chang, W. Li, X. Huang, Z. Wang, X. Chen, X. Qian, R. Guo, Y. Ding, D. Mao, J. Lumin. 130 (2010) 347.
[12] B. Lei, Y. Liu, J. Zhang, J. Meng, S. Man, S. Tan, J. Alloys Compd. 495 (2010) 247.
[13] W. Li, Y. Liu, P. Ai, Mater. Chem. Phys. 119 (2010) 52.
[14] Y. Murazaki, K. Arak, K. Ichinomiya, Rare Earths Jpn. 35 (1999) 41.
[15] X. Wang, Z. Zhang, Z. Tang, Y. Lin, Mater. Chem. Phys. 80 (2003) 1.
[16] J. Zhang, Z. Zhang, Z. Tang, T. Wang, Ceram. Int. 30 (2004) 225.
[17] Y. Wang, Z. Wang, J. Rare Earths 24 (2006) 25.
[18] J. Hölsä, T. Laamanen, M. Lastusaari, M. Malkamäki, J. Niittykoski, E. Zych, Opt. Mater. 31 (2009) 1791.
[19] G. Lakshminarayana, R. Yang, J.R. Qiu, M.G. Brik, G.A. Kumar, I.V. Kityk, J. Phys. D: Appl. Phys. 42 (2009) 015414.
[20] H. Ryu, B.K. Singh, K.S. Bartwal, M.G. Brik, I.V. Kityk, Acta Mater. 56 (2008) 358.
[21] H. Zeng, X. Zhou, L. Zhang, X. Dong, J. Alloys Compd. 460 (2008) 704.
[22] S. Yuan, Y. Yang, B. Fang, G. Chen, Opt. Mater. 30 (2007) 535.
[23] C. Guo, W. Zhang, C. Shi, J. Lumin. 24–25 (1981) 297.
[24] H. Aizawa, T. Katsumata, J. Takahashi, K. Matsunaga, S. Komuro, T. Morikawa, E. Toba, Rev. Sci. Instrum. 74 (2003) 1344.
[25] C.H. Kam, S. Buddhudu, Mater. Lett. 54 (2002) 337.
[26] J.S. Kim, Y.H. Park, S.M. Kim, J.C. Choi, H.L. Park, Solid State Commun. 133 (2005) 445.
[27] C. Guo, L. Luan, C. Chen, D. Huang, Q. Su, Mater. Lett. 62 (2008) 600.
[28] T. Matsuzawa, Y. Aoki, N. Takeuchi, Y. Murayama, J. Electrochem. Soc. 143 (1996) 2670.
[29] H. Yamamoto, T. Matsuzawa, J. Lumin. 72–74 (1997) 287.
[30] T. Katsumata, T. Nabae, K. Sasajima, T. Matsuzawa, J. Cryst. Growth 183 (1998) 361.
[31] E. Nakazawa, H. Yamamoto, J. Lumin. 128 (2008) 494.
[32] C. Liu, G. Che, Phys. Status Solidi (a) 203 (2006) 558.